

# Two-loop Induced Majorana Neutrino Mass in a Radiatively Induced Quark and Lepton Mass Model

Takaaki Nomura<sup>1,\*</sup> and Hiroshi Okada<sup>2,†</sup>

<sup>1</sup>*School of Physics, KIAS, Seoul 130-722, Korea*

<sup>2</sup>*Physics Division, National Center for Theoretical Sciences, Hsinchu, Taiwan 300*

(Dated: May 24, 2019)

## Abstract

A two-loop induced radiative neutrino model is proposed as an extension of our previous work in which the first and second generation standard model fermion masses are generated at one-loop level in both quark and lepton sectors. Then we discuss current neutrino oscillation data, lepton flavor violations, muon anomalous magnetic moment, and a bosonic dark matter candidate, for both the normal and inverted neutrino mass hierarchy. Our numerical analysis shows that less hierarchical Yukawa coupling constants can fit the experimental data with TeV scale dark matter.

Keywords:

---

\*Electronic address: nomura@kias.re.kr

†Electronic address: macokada3hiroshi@cts.nthu.edu.tw

## I. INTRODUCTION

In the standard model (SM), neutrinos and dark matter (DM) candidates are not involved in if the neutrinos could be Majorana property within the renormalizable theory. Radiatively induced mass models are one of the attractive candidates to accommodate these fields, and a lot of groups are trying to establish such models. For example, one-loop induced neutrino mass models are found in Refs. [1], subsequently several variations has been achieved as found in [2]. Two-loop, three-loop, and four-loop models are respectively found in Res. [4], [5], and [6].

Previously we proposed a model in which first and second generation quark and lepton masses are radiatively generated at one-loop level for understanding the mass hierarchy in quark and charged lepton sector [7]. In this model, Dirac type neutrino mass terms are generated in the same way as the other sectors which require a tiny Yukawa coupling as  $O(10^{-13} - 10^{-12})$  due to smallness of neutrino masses. In this paper, we extend the model where the Majorana type active neutrinos are realized at two-loop level. Thus the more natural hierarchy between neutrinos and the other SM fermion sectors can be achieved. Moreover, when neutrinos are Majorana type, it might be clarified through the experiments searching for neutrinoless double beta decay. Also one can predict one of the three neutrinos is massless fermion, because one of the Yukawa couplings is anti-symmetric matrix. This property is the same as the preceding work, i.e., Zee model found in the first reference of the one-loop model. Due to the property, different patterns of allowed regions are obtained depending on normal hierarchy (NH) or inverted hierarchy (IH) of the neutrino masses. In addition, several bosonic DM candidates are involved in and can be detected by direct or indirect detection searches.

This paper is organized as follows. In Sec. II, we show our model, including neutrino sector, LFVs, muon anomalous magnetic moment, and bosonic DM candidate to explain direct detection and relic density. In Sec. III, we have a numerical analysis, and show some results. We conclude and discuss in Sec. IV.

|           | Leptons        |          |          |                |          |          | Bosons(VEVs $\neq$ 0) |           | Bosons(VEVs=0) |               |          |          |
|-----------|----------------|----------|----------|----------------|----------|----------|-----------------------|-----------|----------------|---------------|----------|----------|
| Fields    | $L_L^\alpha$   | $e_R^i$  | $\tau_R$ | $L'_{L,R}^i$   | $N_R^i$  | $N_L^i$  | $\Phi$                | $\varphi$ | $\eta$         | $\Phi_2$      | $S$      | $S^-$    |
| $SU(2)_L$ | <b>2</b>       | <b>1</b> | <b>1</b> | <b>2</b>       | <b>1</b> | <b>1</b> | <b>2</b>              | <b>1</b>  | <b>2</b>       | <b>2</b>      | <b>1</b> | <b>1</b> |
| $U(1)_Y$  | $-\frac{1}{2}$ | -1       | -1       | $-\frac{1}{2}$ | 0        | 0        | $\frac{1}{2}$         | 0         | $\frac{1}{2}$  | $\frac{1}{2}$ | 0        | -1       |
| $U(1)_R$  | 0              | $-x$     | 0        | 0              | $x$      | 0        | 0                     | $x$       | $x$            | $-x$          | 0        | 0        |
| $Z_2$     | +              | +        | +        | -              | -        | -        | +                     | +         | -              | +             | -        | +        |

TABLE I: Field contents of fermions and their charge assignments under  $SU(2)_L \times U(1)_Y \times U(1)_R \times Z_2$ , where each of the flavor index is defined as  $\alpha \equiv 1 - 3$  and  $i = 1, 2$ .

## II. MODEL SETUP

In this section, we review our model and derive formulas for neutrino mass matrix, lepton flavor violations, muon  $g - 2$ , and relic density of DM. The particle contents and their charge assignments are shown in Tab. I, in which only two inert bosons  $\Phi_2$  and  $S^-$  are introduced in addition to the previous work [7] to construct the Majorana type active neutrino masses at the two-loop level. Hence all the phenomenologies except neutrino sector can be retained. Notice here that the inert properties of  $\Phi_2$  assure the local  $U(1)_R$  symmetry even after spontaneous breaking via  $\varphi$ . In addition, since  $\varphi$  and  $\Phi$  as well as all the SM fermions are  $Z_2$  even, the  $Z_2$  symmetry remains after the symmetry breaking where a neutral  $Z_2$  odd particle can be a DM candidate. Notice that we also need  $N_R^i$  which is charged under  $U(1)_R$  to cancel gauge anomaly. Here we assign odd  $Z_2$  charge to  $N_R^i$  in order to eliminate couplings that induce tree- and one-loop level neutrino mass generation in the previous model. In addition, we add  $N_L^i$  to give Dirac mass term like  $M_D \bar{N}_L N_R$  which is generated by  $\varphi \bar{N}_L N_R$  after  $\varphi$  develops a VEV. Due to  $Z_2$  symmetry  $N_{L(R)}$  can be DM candidate, but we omit analysis for  $N_{L(R)}$  DM since it is not related to neutrino mass generation.

Under these symmetries, the relevant Lagrangian and Higgs potential are given by

$$\begin{aligned}
-\mathcal{L} \supset & (y_\ell)_{\alpha j} \bar{L}_\alpha \Phi_2 e_{R_j} + (y'_\ell)_{ij} \bar{L}'_{ij} \eta e_{R_j} + (y_S)_{\alpha j} \bar{L}_\alpha L'_j S + (y'_S)_{\alpha\beta} \bar{L}_\alpha^C (i\sigma_2) L_\beta S^+ \\
& + (y_\tau)_\alpha \bar{L}_\alpha \tau_R (i\sigma_2) \Phi + m_{L'_k} \bar{L}'_k L'_k - \lambda_1 [\Phi^T (i\sigma_2) \Phi_2] \varphi S^- - \lambda_2 (\Phi^\dagger \eta) \varphi^* S + \text{c.c.}, \quad (\text{II.1})
\end{aligned}$$

where  $\sigma_2$  is the Pauli matrix,  $(\alpha, \beta)$  run over  $1 - 3$ ,  $(i, j, k)$  runs over  $1, 2$ , and we abbreviate the full trivial potential. Note that we have the Dirac mass term of  $L'$  since it is introduced as vector-like. In addition, the term with coupling  $y'_S$  is our source of lepton number violation

in generating Majorana neutrino masses. Here we assume that the charged lepton mass is diagonal and we work on the basis where all the coefficients are real and positive for simplicity<sup>1</sup>.

Scalar bosons: In our model, scalar sector has five complex scalar fields  $\{\Phi, \Phi_2, \eta, \varphi, S^\pm\}$  and one real singlet scalar  $S$ . We parametrize the complex scalar fields as follows:

$$\Phi = \begin{bmatrix} w^+ \\ \frac{v+\phi+iz}{\sqrt{2}} \end{bmatrix}, \quad \Phi_2 = \begin{bmatrix} \phi_2^+ \\ \phi_2^- \end{bmatrix}, \quad \eta = \begin{bmatrix} \eta^+ \\ \frac{\eta_R+i\eta_L}{\sqrt{2}} \end{bmatrix}, \quad \varphi \equiv \frac{v' + \varphi_R + iz_R}{\sqrt{2}}, \quad (\text{II.2})$$

where  $v$  ( $\approx 246$  GeV) and  $v'$  are respectively vacuum expectation values (VEVs) of  $\Phi$  and  $\varphi$ , and  $w^\pm$ ,  $z$ , and  $z_R$  are respectively Nambu-Goldstone (NG) bosons which are absorbed by the longitudinal component of  $W$ ,  $Z$ , and  $Z'$  boson. Since each of field set;  $[\varphi, \phi]^T$ ,  $[S, \eta_R]^T$ ,  $[S^\pm, \phi_2^\pm]^T$ , mixes through the terms of  $|\Phi|^2|\varphi|^2$  and  $\lambda_{1,2}$  after developing VEVs of  $\Phi$  and  $\varphi$ , we define the relation between the mass eigenstate and the flavor eigenstate as follow:

$$\begin{aligned} \begin{bmatrix} \varphi \\ \phi \end{bmatrix} &\equiv \begin{bmatrix} \cos a & \sin a \\ -\sin a & \cos a \end{bmatrix} \begin{bmatrix} h_1 \\ h_2 \end{bmatrix}, \quad \begin{bmatrix} S \\ \eta_R \end{bmatrix} \equiv \begin{bmatrix} \cos R & \sin R \\ -\sin R & \cos R \end{bmatrix} \begin{bmatrix} H_1 \\ H_2 \end{bmatrix}, \\ \begin{bmatrix} S^\pm \\ \phi_2^\pm \end{bmatrix} &\equiv \begin{bmatrix} \cos C & \sin C \\ -\sin C & \cos C \end{bmatrix} \begin{bmatrix} H_1^\pm \\ H_2^\pm \end{bmatrix}, \end{aligned} \quad (\text{II.3})$$

where  $h_2$  is the SM Higgs, and we hereafter write  $\sin(\cos)$  as a short hand symbol;  $\sin(\cos) \equiv s(c)$ .

### A. Neutrino mass matrix

The dominant contribution to the active neutrino mass matrix  $m_\nu$  is given at two-loop level where the corresponding diagram is shown in Fig. 1. Calculating the diagram, we

---

<sup>1</sup> The first two columns, which comes from the first and second generations, are induced at the one-loop level. The third column, which corresponds to the third generation, are generated at the tree level. See ref. [7] in details including scalar potential and  $Z'$  boson associated with  $U(1)_R$ .

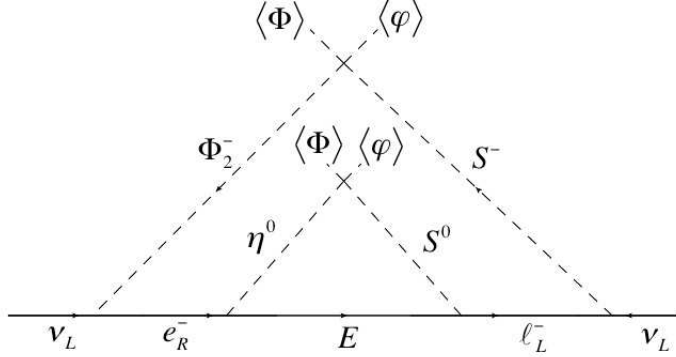


FIG. 1: The two loop diagram for generating Majorana mass term for active neutrinos.

obtain the formula of neutrino mass matrix such that

$$(m_\nu)_{ab} = -s_R c_R s_C c_C \frac{(y_\ell)_{ai}(y'_\ell)_{ij}\mathcal{M}_{E_j}(y_S^\dagger)_{jk}(y'_S)_{kb} + [(y_\ell)_{ai}(y'_\ell)_{ij}\mathcal{M}_{E_j}(y_S^\dagger)_{jk}(y'_S)_{kb}]^T}{2(4\pi)^4}, \quad (\text{II.4})$$

$$\begin{aligned} \mathcal{M}_{E_j} &\equiv m_{L'_j} \int [dx] \int [dX] \frac{y}{(x_4 - 1)^2} \ln \left( \frac{\Delta_3[E_j, H_1^\pm, H_2]\Delta_3[E_j, H_2^\pm, H_1]}{\Delta_3[E_j, H_1^\pm, H_1]\Delta_3[E_j, H_2^\pm, H_2]} \right), \\ \Delta_3[a, b, c] &\equiv xm_a^2 - \frac{y(x_3m_b^2 + x_4m_c^2)}{x_4^2 - x_4}, \\ \int [dx] &\equiv \int_0^1 dx \int_0^{1-x} dy \delta(1 - x - y), \\ \int [dX] &\equiv \int_0^1 dx_1 \int_0^{1-x_1} dx_2 \int_0^{1-x_1-x_2} dx_3 \int_0^{1-x_1-x_2-x_3} x_4 \delta(1 - x_1 - x_2 - x_3 - x_4), \end{aligned} \quad (\text{II.5})$$

where we define  $L' \equiv [E, N]^T$  and its mass is  $m_{L'}$ .

The neutrino mass matrix  $(m_\nu)_{ab}$  can generally be diagonalized by the mixing matrix  $V_{\text{MNS}}$  (PMNS) and written in terms of experimental values depending on the normal hierarchy

(NH) and inverted hierarchy (IH) as follows:

$$(m_\nu)_{ab}^{exp.} = (V_{\text{MNS}} D_\nu V_{\text{MNS}}^T)_{ab}, \quad D_\nu \equiv (m_{\nu_1}, m_{\nu_2}, m_{\nu_3})$$

$$(\text{NH}) : |m_\nu^{exp.}| \approx \begin{bmatrix} 0.0845 - 0.475 & 0.0629 - 0.971 & 0.0411 - 0.964 \\ * & 1.44 - 3.49 & 1.94 - 2.85 \\ * & * & 1.22 - 3.33 \end{bmatrix} \times 10^{-11} \text{ GeV}, \quad (\text{II.6})$$

$$(\text{IH}) : |m_\nu^{exp.}| \approx \begin{bmatrix} 0.993 - 4.96 & 0.00261 - 3.83 & 0.00280 - 3.95 \\ * & 0.00380 - 3.08 & 0.345 - 2.61 \\ * & * & 0.000647 - 3.30 \end{bmatrix} \times 10^{-11} \text{ GeV}, \quad (\text{II.7})$$

$$V_{\text{MNS}} = \begin{bmatrix} c_{13}c_{12} & c_{13}s_{12} & s_{13}e^{-i\delta} \\ -c_{23}s_{12} - s_{23}s_{13}c_{12}e^{i\delta} & c_{23}c_{12} - s_{23}s_{13}s_{12}e^{i\delta} & s_{23}c_{13} \\ s_{23}s_{12} - c_{23}s_{13}c_{12}e^{i\delta} & -s_{23}c_{12} - c_{23}s_{13}s_{12}e^{i\delta} & c_{23}c_{13} \end{bmatrix} \begin{bmatrix} e^{i\alpha_1/2} & 0 & 0 \\ 0 & e^{i\alpha_2/2} & 0 \\ 0 & 0 & 1 \end{bmatrix},$$

$$(\text{II.8})$$

where we have used the following neutrino oscillation data at  $3\sigma$  [8] given by

$$(\text{NH}) : 0.278 \leq s_{12}^2 \leq 0.375, \quad 0.392 \leq s_{23}^2 \leq 0.643, \quad 0.0177 \leq s_{13}^2 \leq 0.0294, \quad \delta \in [-\pi, \pi],$$

$$m_{\nu_3} = (\sqrt{23.0} - \sqrt{26.5}) \times 10^{-11} \text{ GeV}, \quad m_{\nu_2} = (\sqrt{0.711} - \sqrt{0.818}) \times 10^{-11} \text{ GeV},$$

$$(\text{II.9})$$

$$(\text{IH}) : 0.278 \leq s_{12}^2 \leq 0.375, \quad 0.403 \leq s_{23}^2 \leq 0.640, \quad 0.0183 \leq s_{13}^2 \leq 0.0297, \quad \delta \in [-\pi, \pi],$$

$$m_{\nu_1} = (\sqrt{22} - \sqrt{25.4}) \times 10^{-11} \text{ GeV}, \quad m_{\nu_2} = (\sqrt{22.711} - \sqrt{26.218}) \times 10^{-11} \text{ GeV},$$

$$(\text{II.10})$$

and Majorana phases  $\alpha_{1,2}$  taken to be  $\alpha_{1,2} \in [-\pi, \pi]$  for both cases. Notice here that we assume to be normal ordering to obtain the above numerical value of the neutrino mass matrix, and we take one of three neutrino masses is zero, which is predicted by the theoretical aspect that  $y'_S$  is anti-symmetric matrix, therefore the rank of neutrino mass matrix is reduced to two. Applying the above nature, we can rewrite two components of  $y'_S$  in terms

of experimental values and one of the component of  $y'_S$  as follows <sup>2</sup>:

$$(\text{NH}) : (y'_S)_{e\tau} = \left( \frac{s_{12}c_{23}}{c_{12}c_{13}} + \frac{s_{13}s_{23}}{c_{13}} e^{-i\delta} \right) (y'_S)_{\mu\tau}, \quad (y'_S)_{e\mu} = \left( \frac{s_{12}c_{23}}{c_{12}c_{13}} - \frac{s_{13}s_{23}}{c_{13}} e^{-i\delta} \right) (y'_S)_{\mu\tau}, \quad (\text{II.11})$$

$$(\text{IH}) : (y'_S)_{e\tau} = -\frac{s_{23}}{t_{13}} (y'_S)_{\mu\tau}, \quad (y'_S)_{e\mu} = \frac{c_{23}}{t_{13}} (y'_S)_{\mu\tau}, \quad (\text{II.12})$$

where the explicit form of  $y'_S$  is given by

$$(y'_S) \equiv \begin{bmatrix} 0 & (y'_S)_{e\mu} & (y'_S)_{e\tau} \\ -(y'_S)_{e\mu} & 0 & (y'_S)_{\mu\mu} \\ -(y'_S)_{e\tau} & -(y'_S)_{\mu\tau} & 0 \end{bmatrix}. \quad (\text{II.13})$$

In our numerical analysis, only  $(y'_S)_{\mu\tau}$  is an input parameter, and we will search the allowed region of our parameter space by comparing the experimental values in Eqs. (II.6) and (II.7).

## B. Lepton Flavor Violations (LFVs) and muon anomalous magnetic moment

*Lepton Flavor Violations:* The Yukawa couplings can induce LFV processes at loop level. Here we focus on  $\ell_b \rightarrow \ell_a \gamma$  processes at one-loop level where  $H_i$  and  $E$  run inside a loop, and its branching ratio is written as

$$\text{BR}(\ell_i \rightarrow \ell_j \gamma) = \frac{48\pi^3 C_i \alpha_{\text{em}}}{G_F^2 m_i^2} (|(a_R)_{ij}|^2 + |(a_L)_{ij}|^2), \quad (\text{II.14})$$

where  $\alpha_{\text{em}} \approx 1/137$  is the fine-structure constant,  $C_b = (1, 1/5)$  for  $(b = \mu, \tau)$ ,  $G_F \approx 1.17 \times 10^{-5} \text{ GeV}^{-2}$  is the Fermi constant. Calculating loop diagrams,  $a_L$  and  $a_R$  are respectively

---

<sup>2</sup> The detail analysis is found in ref. [9] for both hierarchies.

| Process                           | $(i, j)$ | Experimental bounds (90% CL)                          | References |
|-----------------------------------|----------|---|------------|
| $\mu^- \rightarrow e^- \gamma$    | (2, 1)   | $BR(\mu \rightarrow e\gamma) < 4.2 \times 10^{-13}$   | [10]       |
| $\tau^- \rightarrow e^- \gamma$   | (3, 1)   | $Br(\tau \rightarrow e\gamma) < 3.3 \times 10^{-8}$   | [11]       |
| $\tau^- \rightarrow \mu^- \gamma$ | (3, 2)   | $BR(\tau \rightarrow \mu\gamma) < 4.4 \times 10^{-8}$ | [11]       |

TABLE II: Summary of  $\ell_i \rightarrow \ell_j \gamma$  process and the upper bound of experimental data.

given as

$$\begin{aligned}
a_R &\equiv a_{R_0} + a_{R_1} + a_{R_2}, \quad a_L \equiv a_{L_1} + a_{L_2}, \\
(a_{R_0})_{ij} &= -\frac{s_R c_R}{2\sqrt{2}(4\pi)^2} \sum_{k=1}^3 (y'_\ell)_{j,k} m_{L'_k} (y_S)_{k,i} (F_1[H_1, E_k] - F_1[H_2, E_k]), \\
(a_{R_1})_{ij} &= -\frac{1}{2\sqrt{2}(4\pi)^2} \sum_{k=1}^3 \left[ \frac{2m_i(y_\ell)_{j,k}(y_\ell^\dagger)_{k,i}}{m_{\phi_2}^2} - [m_j(y_\ell)_{j,k}^\dagger(y_\ell)_{k,i} + m_i(y'_S)_{j,k}^\dagger(y'_S)_{k,i}] \left( \frac{c_C^2}{m_{H_1}^\pm} + \frac{s_C^2}{m_{H_2}^\pm} \right) \right], \\
(a_{R_2})_{ij} &= \frac{1}{(4\pi)^2} \sum_{k=1}^3 \left( (y'_\ell)_{j,k}^\dagger m_j(y'_\ell)_{k,i} F_2[E_k, \eta_\pm] - (y_S)_{j,k}^\dagger m_i(y_S)_{k,i} (c_R^2 F_2[H_1, E_k] + s_R^2 F_2[H_2, E_k]) \right), \\
(a_{L_1})_{ij} &= -\frac{1}{2\sqrt{2}(4\pi)^2} \sum_{k=1}^3 \left[ \frac{2m_j(y_\ell)_{j,k}(y_\ell^\dagger)_{k,i}}{m_{\phi_2}^2} - [m_i(y_\ell)_{j,k}^\dagger(y_\ell)_{k,i} + m_i(y'_S)_{j,k}^\dagger(y'_S)_{k,i}] \left( \frac{c_C^2}{m_{H_1}^\pm} + \frac{s_C^2}{m_{H_2}^\pm} \right) \right], \\
(a_{L_2})_{ij} &= \frac{1}{(4\pi)^2} \sum_{k=1}^3 \left( (y'_\ell)_{j,k}^\dagger m_i(y'_\ell)_{k,i} F_2[E_k, \eta_\pm] - (y_S)_{j,k}^\dagger m_j(y_S)_{k,i} (c_R^2 F_2[H_1, E_k] + s_R^2 F_2[H_2, E_k]) \right),
\end{aligned} \tag{II.15}$$

where

$$\begin{aligned}
F_1[a, b] &\equiv \frac{3m_a^4 - 4m_a^2 m_b^2 + m_b^4 + 2m_a^4 \ln(m_b^2/m_a^2)}{2(m_a^2 - m_b^2)^3}, \quad F_1[a, a(=b)] \equiv -\frac{1}{3m_a^2}. \\
F_2[a, b] &\equiv \frac{2m_a^6 + 3m_a^4 m_b^2 - 6m_a^2 m_b^4 + m_b^6 + 12m_a^4 m_b^2 \ln(m_b/m_a)}{12(m_a^2 - m_b^2)^4}, \quad F_2[a, a(=b)] \equiv \frac{1}{24m_a^2}.
\end{aligned} \tag{II.16}$$

Here each of the experimental bound is summarized in table II, and we impose these constraints in our numerical analysis.

*Muon anomalous magnetic moment:* Our formula of muon  $g - 2$  can be written in terms of  $a_L$  and  $a_R$ , which have been derived in LFV sector as follows:

$$\Delta a_\mu \approx -m_\mu (a_R + a_L)_{22}, \tag{II.17}$$

where the lower index 2 of  $a_{R(L)}$  represents the muon.

### C. Dark Matter

Here we identify DM as  $H_1 (\equiv X)$  since it is correlated to neutrino mass matrix and LFVs. Then we provide formulas of nucleon-DM scattering cross section for the direct detection search and relic density which are taken into account in our numerical analysis later.

*Direct detection:* We have a spin independent scattering cross section with nucleon through  $h_{1,2}$  portal processes and its form is given by

$$\sigma_N \approx 0.082 \frac{m_N^4}{\pi v^2 M_X^2} \left( \frac{\mu_{2Xh_1}}{m_{h_1}^2} + \frac{\mu_{2Xh_2}}{m_{h_2}^2} \right)^2, \quad (\text{II.18})$$

where  $\mu_{2Xh_i}$  is the trilinear coupling of  $X - X - h_i (i = 1, 2)$ , and the mass of nucleon, which is symbolized by  $m_N$ , is around 0.939 GeV. Recent LUX experiment in 2016 reported the lower bound on  $\sigma_N \lesssim 2.2 \times 10^{-46} \text{ cm}^2$  at 50 GeV mass range of DM at the 90 % confidential level [12].

*Relic density:* Our relevant processes for the thermally averaged cross section comes from  $2X \rightarrow 2h_2$ ,  $2X \rightarrow f\bar{f} (f \approx top)$ , and  $2X \rightarrow VV^* (V = Z, W^\pm)$ <sup>3</sup>. Here we note that when  $s_R$  is not much small,  $m_X \simeq m_{H_2} \simeq m_{\eta^\pm}$  is required for TeV scale DM due to large contribution from  $VV^*$  channel without mass degeneration [13], and co-annihilation processes should be taken into account. In our numerical analysis below, we take small  $s_R$  so that wider range of  $m_{H_2}$  and  $m_{\eta^\pm}$  are allowed, and mass ranges outside co-annihilation region are discussed. The squared amplitude for relevant processes and the approximated formula of relic density are given by [14, 15]

$$\sigma v_{\text{rel}} \approx \int_0^\pi \sin \theta d\theta \frac{|\bar{M}|^2}{16\pi s} \sqrt{1 - \frac{4m_f^2}{s}}, \quad (\text{II.19})$$

---

<sup>3</sup> From the analysis of neutrino oscillation and LFVs, all the Yukawa couplings are so tiny that the cross section coming from Yukawas are negligible.

where

$$|\bar{M}|^2 \approx |\bar{M}(2X \rightarrow 2h_2)|^2 + |\bar{M}(2X \rightarrow t\bar{t})|^2 + |\bar{M}(2X \rightarrow VV^*)|^2, \quad (\text{II.20})$$

$$\begin{aligned} |\bar{M}(2X \rightarrow 2h_2)|^2 &= \frac{1}{2} \left| \lambda_{2X2h_2} + \frac{\mu_{2Xh_1}\mu_{2h_2h_1}}{s - m_{h_1}^2} + \frac{\mu_{2Xh_2}\mu_{2h_2h_2}}{s - m_{h_2}^2} \right. \\ &\quad \left. + \mu_{Xh_1h_1}^2 \left( \frac{1}{t - m_{h_1}^2} + \frac{1}{u - m_{h_1}^2} \right) + \mu_{Xh_1h_2}^2 \left( \frac{1}{t - m_{h_2}^2} + \frac{1}{u - m_{h_2}^2} \right) \right|^2, \end{aligned} \quad (\text{II.21})$$

$$|\bar{M}(2X \rightarrow t\bar{t})|^2 = 6 \left( \frac{m_t}{v} \right)^2 \left| \frac{\mu_{2Xh_1}}{s - M_{h_1}^2} + \frac{\mu_{2Xh_2}}{s - M_{h_2}^2} \right|^2 (s - 4m_t^2), \quad (\text{II.22})$$

$$|\bar{M}(2X \rightarrow 2Z)|^2 = \frac{g_Z^4}{4} G_{\mu\nu}^Z G_{\alpha\beta}^Z \left( -g_{\mu\alpha} + \frac{k_{1\mu}k_{1\alpha}}{m_Z^2} \right) \left( -g_{\nu\beta} + \frac{k_{2\nu}k_{2\beta}}{m_Z^2} \right), \quad (\text{II.23})$$

$$|\bar{M}(2X \rightarrow W^+W^-)|^2 = \frac{g_2^4}{4} G_{\mu\nu}^W G_{\alpha\beta}^W \left( -g_{\mu\alpha} + \frac{k_{1\mu}k_{1\alpha}}{m_W^2} \right) \left( -g_{\nu\beta} + \frac{k_{2\nu}k_{2\beta}}{m_W^2} \right),$$

$$\begin{aligned} G_{ab}^V &\equiv g_{ab} \left( s_R^2 - \frac{s_a v \mu_{2Xh_1}}{s - m_{h_1}^2} + \frac{c_a v \mu_{2Xh_2}}{s - m_{h_2}^2} \right) \\ &\quad + \frac{s_R^2}{2} \left( \frac{(2p_1 - k_1)_a(p_2 - p_1 + k_1)_b}{t - m_{\eta_V}^2} + \frac{(2p_1 - k_2)_a(p_2 - p_1 + k_2)_b}{u - m_{\eta_V}^2} \right), \end{aligned} \quad (\text{II.24})$$

where  $m_{\eta_Z} \equiv m_{\eta_I}$ ,  $m_{\eta_W} \equiv m_{\eta^\pm}$ ,  $p_{1,2}$  and  $k_{1,2}$  are respectively the momentum of the initial and final state fields, and a trilinear coupling  $\mu$  can be written in terms of quartic couplings and VEVs. Then the relic density is given by

$$\Omega h^2 \approx \frac{1.07 \times 10^9 x_f^2}{g_*^{1/2} M_{\text{pl}}[\text{GeV}] (a_{\text{eff}} x_f + 3b_{\text{eff}})}, \quad (\text{II.25})$$

where  $g_* \approx 100$  is the total number of effective relativistic degrees of freedom at the time of freeze-out,  $M_{\text{pl}} = 1.22 \times 10^{19} [\text{GeV}]$  is Planck mass,  $x_f \approx 25$ , and  $a_{\text{eff}}$  and  $b_{\text{eff}}$  are derived by expanding  $\sigma v_{\text{rel}}$  in terms of  $v_{\text{rel}}$  up to  $v_{\text{rel}}^2$  as

$$\sigma v_{\text{rel}} \approx a_{\text{eff}} + b_{\text{eff}} v_{\text{rel}}^2. \quad (\text{II.26})$$

The observed relic density reported by Planck suggest that  $\Omega h^2 \approx 0.12$  [16].

### III. NUMERICAL RESULTS

In this section, we carry out numerical analysis to search for the parameter region which can fit the experimental data. To reduce number of free parameters, we first fix some parameters as follows;  $s_a = 0.3$ ,  $s_R = 0.1$ ,  $s_C = 1$ ,  $m_{h_1} = 4$  TeV. We next randomly select values of masses as  $M_X \in [0, 10]$  TeV,  $m_{\phi_2} \in [11M_X/10, 9]$  TeV,  $m_{H_2^\pm} \in [11M_X/10, 12M_X/10]$

TeV,  $\mu_{2Xh_i} = \mu_{2h_2h_i} = \mu_{Xh_2h_i} \equiv \mu \in [10^{-4}, 10^{-3}]$  GeV,<sup>4</sup>  $m_{L'_1} \in [11M_X/10, 9]$  TeV,  $m_{L'_2} \in [m_{L'_1}, 9.5]$  TeV,  $m_{L'_3} \in [m_{L'_2}, 10]$  TeV, and  $m_{\eta^\pm} = m_{H_2} \in [11M_X/10, 12(11.1)M_X/10]$ , where we consider the mass range of  $m_{H_\eta^\pm}$  and  $m_{H_2}$  outside co-annihilation region [14] as discussed above. Then, we randomly select values of the 29 parameters within  $[-1, 1]$  for all the dimensionless couplings to search for allowed parameter region.<sup>5</sup> As a result we find the allowed ranges for both NH and IH cases as follows:

$$(y'_S)_{\mu\tau} \in [-0.027, 0.027], \quad \lambda_{2X2h_2} \in [0.1, 1], \quad (\text{III.1})$$

$$y_S = \begin{bmatrix} 0.01 - 0.135 & -(0.025 - 0.02) & -(0.0265 - 0.02) \\ 0.03 - 0.036 & 0.01 - 0.015 & -(0.045 - 0.04) \\ -(0.027 - 0.02) & -(0.0208 - 0.02) & -(0.028 - 0.02) \end{bmatrix},$$

$$y_\ell = \begin{bmatrix} -(0.016 - 0.01) & 0.04 - 0.0453 & -(0.02 - 0.01) \\ -(0.0063 - 0.001) & 0.04 - 0.05 & -(0.031 - 0.01) \\ 0.001 - 0.0012 & -(0.0174 - 0.01) & 0.03 - 0.036 \end{bmatrix},$$

$$y'_\ell = \begin{bmatrix} 0.03 - 0.037 & -(0.0445 - 0.04) & 0.001 - 0.0088 \\ 0.01 - 0.0123 & 0.02 - 0.0275 & -(0.032 - 0.01) \\ 0.01 - 0.03 & 0.001 - 0.0094 & 0.001 - 0.005 \end{bmatrix}, \quad (\text{III.2})$$

which can reproduce neutrino oscillation data, satisfies the constraints from LFVs and the direct detection searches<sup>6</sup> and can provide the observed relic density of DM;  $0.11 \leq \Omega h^2 \leq 0.13$ . Here  $\lambda_{2X2h_2}$  is the coupling constants of four point interaction  $X-X-h_2-h_2$ . We thus find that the hierarchy of the required Yukawa coupling constants is not large. For the parameter ranges, we generate  $5 \times 10^4$  million sample points and make figures to describe some correlations. The plots at the left-upper (NH) and the right-upper (IH) in Fig. 2 represent the allowed region in terms of the DM mass and the muon  $g - 2$ . The red region is the case of  $m_{\eta^\pm} = m_{H_2} \in [11M_X/10, 12M_X/10]$ , and the maximum value of muon  $g - 2$  reaches  $\mathcal{O}(1.0 \times 10^{-13})$  for NH and  $\mathcal{O}(4.0 \times 10^{-13})$  for IH. On the other hands the blue one is the case

<sup>4</sup> Notice here that the upper value  $10^{-3}$  for  $\mu_{2Xh_i}$  is required to evade the constraint from the direct detection search, and other trilinear couplings are taken to be the same value for simplicity. When we relax the relation applying larger  $\mu_{2h_2h_i}$  and  $\mu_{Xh_2h_i}$ , we have larger DM annihilation cross section reducing relic density without affecting neutrino mass matrix.

<sup>5</sup> Totally we have 45(16 mass dimensions plus 29 dimensionless) input parameters, and 23 output parameters.

<sup>6</sup> We conservatively take the constraint  $\sigma_N \lesssim 10^{-45} \text{cm}^2$  for all the mass region of DM.

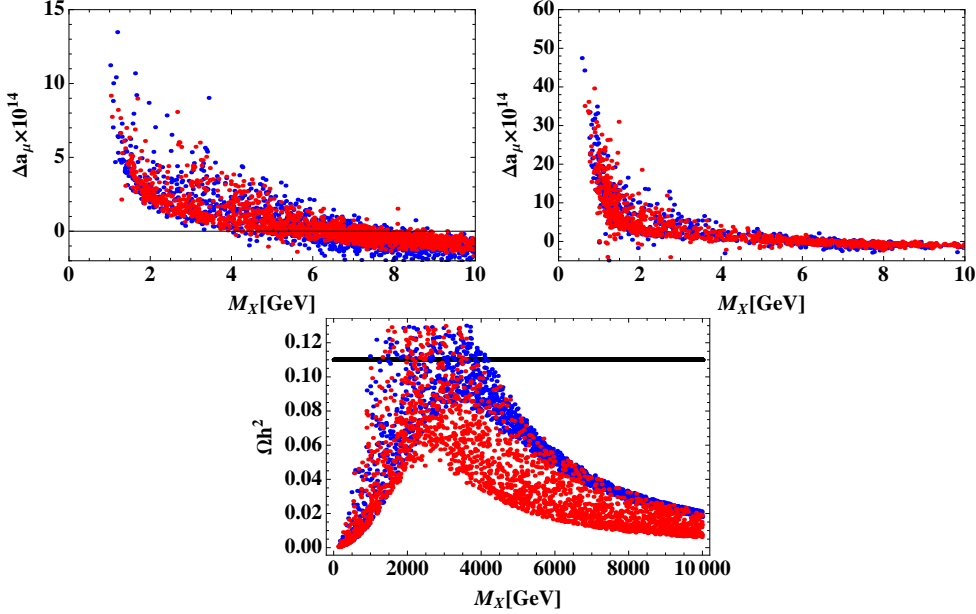


FIG. 2: The plots at the left-upper (NH) and the right-upper (IH) represent the allowed region in terms of the DM mass and the muon  $g - 2$ . The red region is the case of  $m_{\eta^\pm} = m_{H_2} \in [11M_X/10, 12M_X/10]$ , and the maximum value of muon  $g - 2$  reaches  $\mathcal{O}(1.0 \times 10^{-13})$  for NH and  $\mathcal{O}(4.0 \times 10^{-13})$  for IH. On the other hand the blue one is the case of  $m_{\eta^\pm} = m_{H_2} \in [11M_X/10, 11.1M_X/10]$ , and the maximum value of muon  $g - 2$  reaches  $\mathcal{O}(1.5 \times 10^{-13})$  for NH and  $\mathcal{O}(5.0 \times 10^{-13})$  for IH. One also find that the lower bound of the DM mass to be  $1000 \text{ GeV} \lesssim M_X$ , which comes from the LFVs for both cases. The plot at the bottom represents the allowed region in terms of the DM mass and its relic density. The red region and blue region correspond to the same parameter setting as the upper figures. These analyses give the constraints on the DM mass and  $\Delta a_\mu$ ;  $1000 \text{ GeV} \lesssim M_X \lesssim 4500 \text{ GeV}$ , and  $0 \lesssim \Delta a_\mu \lesssim (1 - 1.5) \times 10^{-13}$  for NH and  $0 \lesssim \Delta a_\mu \lesssim (4 - 5) \times 10^{-13}$  for IH.

of  $m_{\eta^\pm} = m_{H_2} \in [11M_X/10, 11.1M_X/10]$ , and the maximum value of muon  $g - 2$  reaches  $\mathcal{O}(1.5 \times 10^{-13})$  for NH and  $\mathcal{O}(5.0 \times 10^{-13})$  for IH. One also find that the lower bound of the DM mass to be  $1000 \text{ GeV} \lesssim M_X$ , which comes from the LFVs for both cases. Notice here that the muon  $g - 2$  is much smaller than the current experimental value  $\mathcal{O}(10^{-9})$  [17].

The plot at the bottom in Fig. 2 represents the allowed region in terms of the DM mass and its relic density. The red region and blue region corresponds to the same parameter setting as the upper plots in Fig. 2. This analysis gives the definite constraint on the DM

mass;  $1000 \text{ GeV} \lesssim M_X \lesssim 4500 \text{ GeV}$ . When the degeneracy between  $M_X$  and  $m_{\eta^\pm}$  relaxes, one finds that the bond of allowed region becomes to be wider. Notice here that it does not affect to the neutrino mass ordering because Yukawa couplings are neglected to the relic density. For the lower range of the DM mass, the relic density decreases due to increasing annihilation cross section whose dominant mode is  $2X \rightarrow 2h$ . On the other hand, DM relic density decreases in the allowed regions with the larger DM mass, which comes from larger annihilation cross section for  $2X \rightarrow VV^*$  mode; it seems to violate the unitarity bound, however, this curve becomes flat in the limit  $M_X \rightarrow \infty$ .

Accommodating the result of  $1000 \text{ GeV} \lesssim M_X \lesssim 4500 \text{ GeV}$  and feeding it back into the first figure, we also find the lower bound of muon  $g - 2$  that tells the negative value does not tend to be allowed. In summary of our numerical analysis, we find as follows:

$$1000 \text{ GeV} \lesssim M_X \lesssim 4500 \text{ GeV}, \quad (\text{III.3})$$

$$(\text{NH}) : 0 \lesssim \Delta a_\mu \lesssim 1.0 \times 10^{-13} \text{ for } m_{\eta^\pm} = m_{H_2} \in [11M_X/10, 12M_X/10], \quad (\text{III.4})$$

$$0 \lesssim \Delta a_\mu \lesssim 1.5 \times 10^{-13} \text{ for } m_{\eta^\pm} = m_{H_2} \in [11M_X/10, 11.1M_X/10], \quad (\text{III.5})$$

$$(\text{IH}) : 0 \lesssim \Delta a_\mu \lesssim 4.0 \times 10^{-13} \text{ for } m_{\eta^\pm} = m_{H_2} \in [11M_X/10, 12M_X/10], \quad (\text{III.6})$$

$$0 \lesssim \Delta a_\mu \lesssim 5.0 \times 10^{-13} \text{ for } m_{\eta^\pm} = m_{H_2} \in [11M_X/10, 11.1M_X/10]. \quad (\text{III.7})$$

It is worthwhile mentioning that lager value of muon  $g - 2$  tends to be obtained by the IH case. One of the main reason is that the value of  $(y'_S)_{e\mu}$ , which contributes not to the constraint of  $\mu \rightarrow e\gamma$  but to do the muon  $g - 2$ , tends to be larger than the NH case as shown in Fig. 3 due to the relation between  $y'_S$  in Eqs. (II.11) and (II.12).

#### IV. CONCLUSIONS AND DISCUSSIONS

We have studied a two-loop induced radiative neutrino model as an extension of our previous work in which the first and second generation standard model fermion masses in all the sector are induced at one-loop level. Then we have discussed current neutrino oscillation data, lepton flavor violations, muon anomalous magnetic moment, and a bosonic dark matter candidate explaining the relic density under the direct detection constraint, considering both the normal and inverted neutrino mass hierarchy. We have found that less hierarchical Yukawa couplings can fit the neutrino oscillation data satisfying the constrains from LFVs. Then we have found some results in terms of the DM mass, the muon  $g - 2$

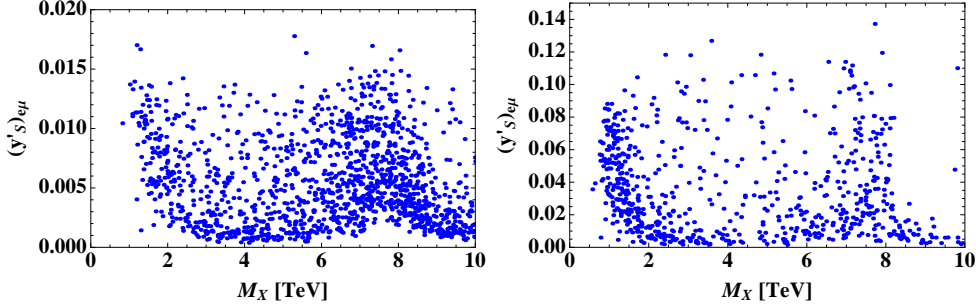


FIG. 3: The left figure (NH) and the right one (IH) represent the allowed region in terms of the DM mass and  $(y'_S)_{e\mu}$ . These figure tell us that its scale of IH is about ten times as large as the one of NH, where  $m_{\eta^\pm} = m_{H_2} \in [11M_X/10, 12M_X/10]$  is used for both case, since its scale does not depend on the degeneracy.

$(\Delta a_\mu)$  where DM mass is in the range of 1 TeV to 4.5 TeV, and  $0 \lesssim \Delta a_\mu \lesssim 1.0(1.5) \times 10^{-13}$  with  $m_{\eta^\pm} = m_{H_2} \in [11M_X/10, 12(11.1)M_X/10]$  in NH case while  $0 \lesssim \Delta a_\mu \lesssim 4.0(5.0) \times 10^{-13}$  with  $m_{\eta^\pm} = m_{H_2} \in [11M_X/10, 12(11.1)M_X/10]$  in IH case. In addition the key component of the anti-symmetric Yukawa coupling  $y'_S$  can be order of  $\sim 0.01(0.1)$  for NH(IH) cases. It is worthwhile mentioning that larger value of muon  $g - 2$  tends to be obtained by the IH case. One of the main reason is that the value of  $(y'_S)_{e\mu}$ , which contributes not to the constraint of  $\mu \rightarrow e\gamma$  but to do the muon  $g - 2$ , tends to be larger than the NH case as shown in Fig. 3 due to the relation between  $y'_S$  in Eqs. (II.11) and (II.12). Especially we have found that IH is in favor of the muon  $g - 2$  although the maximum value is still smaller than the current experimental result.

### Acknowledgments

H. O. is sincerely grateful for all the KIAS members, Korean cordial persons, foods, culture, weather, and all the other things.

---

[1] A. Zee, Phys. Lett. B **93**, 389 (1980) [Erratum-ibid. B **95**, 461 (1980)]; T. P. Cheng and L. F. Li, Phys. Rev. D **22**, 2860 (1980); A. Pilaftsis, Z. Phys. C **55**, 275 (1992) doi:10.1007/BF01482590

[hep-ph/9901206]; E. Ma, Phys. Rev. D **73**, 077301 (2006) [hep-ph/0601225].

- [2] P. -H. Gu and U. Sarkar, Phys. Rev. D **77**, 105031 (2008) [arXiv:0712.2933 [hep-ph]]; N. Sahu and U. Sarkar; Phys. Rev. D **78**, 115013 (2008) [arXiv:0804.2072 [hep-ph]]; P. -H. Gu and U. Sarkar, Phys. Rev. D **78**, 073012 (2008) [arXiv:0807.0270 [hep-ph]]; D. Aristizabal Sierra and D. Restrepo, JHEP **0608**, 036 (2006) [hep-ph/0604012]; R. Bouchand and A. Merle, JHEP **1207**, 084 (2012) [arXiv:1205.0008 [hep-ph]]; K. L. McDonald, JHEP **1311**, 131 (2013) [arXiv:1310.0609 [hep-ph]]; E. Ma, Phys. Lett. B **732**, 167 (2014) [arXiv:1401.3284 [hep-ph]]; Y. Kajiyama, H. Okada and K. Yagyu, Nucl. Phys. B **887**, 358 (2014) [arXiv:1309.6234 [hep-ph]]; S. Kanemura, O. Seto and T. Shimomura, Phys. Rev. D **84**, 016004 (2011) [arXiv:1101.5713 [hep-ph]]; S. Kanemura, T. Nabeshima and H. Sugiyama, Phys. Lett. B **703**, 66 (2011) [arXiv:1106.2480 [hep-ph]]; S. Kanemura, T. Nabeshima and H. Sugiyama, Phys. Rev. D **85**, 033004 (2012) [arXiv:1111.0599 [hep-ph]]; D. Schmidt, T. Schwetz and T. Toma, Phys. Rev. D **85**, 073009 (2012) [arXiv:1201.0906 [hep-ph]]; S. Kanemura and H. Sugiyama, Phys. Rev. D **86**, 073006 (2012) [arXiv:1202.5231 [hep-ph]]; Y. Farzan and E. Ma, Phys. Rev. D **86**, 033007 (2012) [arXiv:1204.4890 [hep-ph]]; K. Kumericki, I. Picek and B. Radovcic, JHEP **1207**, 039 (2012) [arXiv:1204.6597 [hep-ph]]; K. Kumericki, I. Picek and B. Radovcic, Phys. Rev. D **86**, 013006 (2012) [arXiv:1204.6599 [hep-ph]]; E. Ma, Phys. Lett. B **717**, 235 (2012) [arXiv:1206.1812 [hep-ph]]; G. Gil, P. Chankowski and M. Krawczyk, Phys. Lett. B **717**, 396 (2012) [arXiv:1207.0084 [hep-ph]]; H. Okada and T. Toma, Phys. Rev. D **86**, 033011 (2012) arXiv:1207.0864 [hep-ph]; D. Hehn and A. Ibarra, Phys. Lett. B **718**, 988 (2013) [arXiv:1208.3162 [hep-ph]]; P. S. B. Dev and A. Pilaftsis, Phys. Rev. D **86**, 113001 (2012) [arXiv:1209.4051 [hep-ph]]; Y. Kajiyama, H. Okada and T. Toma, Eur. Phys. J. C **73**, 2381 (2013) [arXiv:1210.2305 [hep-ph]]; T. Toma and A. Vicente, JHEP **1401**, 160 (2014) [arXiv:1312.2840, arXiv:1312.2840 [hep-ph]]; S. Kanemura, T. Matsui and H. Sugiyama, Phys. Lett. B **727**, 151 (2013) [arXiv:1305.4521 [hep-ph]]; S. S. C. Law and K. L. McDonald, JHEP **1309**, 092 (2013) [arXiv:1305.6467 [hep-ph]]; S. Baek and H. Okada, arXiv:1403.1710 [hep-ph]; S. Kanemura, T. Matsui and H. Sugiyama, Phys. Rev. D **90**, 013001 (2014) [arXiv:1405.1935 [hep-ph]]; S. Fraser, E. Ma and O. Popov, Phys. Lett. B **737**, 280 (2014) [arXiv:1408.4785 [hep-ph]]; A. Vicente and C. E. Yaguna, JHEP **1502**, 144 (2015) [arXiv:1412.2545 [hep-ph]]; S. Baek, H. Okada and K. Yagyu, JHEP **1504**, 049 (2015) [arXiv:1501.01530 [hep-ph]]; A. Merle and M. Platscher, Phys. Rev. D **92**, no. 9, 095002

(2015) [arXiv:1502.03098 [hep-ph]]; D. Restrepo, A. Rivera, M. Sánchez-Peláez, O. Zapata and W. Tangarife, arXiv:1504.07892 [hep-ph]; A. Merle and M. Platscher, JHEP **1511**, 148 (2015) [arXiv:1507.06314 [hep-ph]]; W. Wang and Z. L. Han, Phys. Rev. D **92**, 095001 (2015) [arXiv:1508.00706 [hep-ph]]; Y. H. Ahn and H. Okada, Phys. Rev. D **85**, 073010 (2012) [arXiv:1201.4436 [hep-ph]]; E. Ma, A. Natale and A. Rashed, Int. J. Mod. Phys. A **27**, 1250134 (2012) [arXiv:1206.1570 [hep-ph]]; A. E. Carcamo Hernandez, I. d. M. Varzielas, S. G. Kovalenko, H. Päs and I. Schmidt, Phys. Rev. D **88**, 076014 (2013) [arXiv:1307.6499 [hep-ph]]; E. Ma and A. Natale, Phys. Lett. B **723**, 403 (2014) [arXiv:1403.6772 [hep-ph]]; E. Ma, Phys. Lett. B **741**, 202 (2015) [arXiv:1411.6679 [hep-ph]]; E. Ma, arXiv:1504.02086 [hep-ph]; E. Ma, Phys. Rev. Lett. **112**, 091801 (2014) [arXiv:1311.3213 [hep-ph]]; H. Okada and K. Yagyu, Phys. Rev. D **89**, 053008 (2014) [arXiv:1311.4360 [hep-ph]]; H. Okada and K. Yagyu; Phys. Rev. D **90**, no. 3, 035019 (2014) [arXiv:1405.2368 [hep-ph]], V. Brdar, I. Picek and B. Radovcic, Phys. Lett. B **728**, 198 (2014) [arXiv:1310.3183 [hep-ph]]; H. Okada, Y. Orikasa and T. Toma, arXiv:1511.01018 [hep-ph]; F. Bonnet, M. Hirsch, T. Ota and W. Winter, JHEP **1207**, 153 (2012) [arXiv:1204.5862 [hep-ph]]; F. R. Joaquim and J. T. Penedo, Phys. Rev. D **90**, no. 3, 033011 (2014) [arXiv:1403.4925 [hep-ph]]; H. Davoudiasl and I. M. Lewis, Phys. Rev. D **90**, no. 3, 033003 (2014) [arXiv:1404.6260 [hep-ph]]; M. Lindner, S. Schmidt and J. Smirnov, arXiv:1405.6204 [hep-ph]; H. Okada and Y. Orikasa, arXiv:1412.3616 [hep-ph]; Y. Mambrini, S. Profumo and F. S. Queiroz, arXiv:1508.06635 [hep-ph]; S. M. Boucenna, S. Morisi and J. W. F. Valle, Adv. High Energy Phys. **2014**, 831598 (2014) [arXiv:1404.3751 [hep-ph]]; A. Ahriche, S. M. Boucenna and S. Nasri, arXiv:1601.04336 [hep-ph]; S. Fraser, C. Kownacki, E. Ma and O. Popov, arXiv:1511.06375 [hep-ph]; S. Fraser, E. Ma and M. Zakeri, arXiv:1511.07458 [hep-ph]; R. Adhikari, D. Borah and E. Ma, arXiv:1512.05491 [hep-ph]; H. Okada and Y. Orikasa, arXiv:1512.06687 [hep-ph]; A. Ibarra, C. E. Yaguna and O. Zapata, Phys. Rev. D **93**, no. 3, 035012 (2016) [arXiv:1601.01163 [hep-ph]]; C. Arbelaez, A. E. C. Hernandez, S. Kovalenko and I. Schmidt, arXiv:1602.03607 [hep-ph]; A. Ahriche, K. L. McDonald, S. Nasri and I. Picek, Phys. Lett. B **757**, 399 (2016) [arXiv:1603.01247 [hep-ph]]; W. B. Lu and P. H. Gu, arXiv:1603.05074 [hep-ph]; C. Kownacki and E. Ma, arXiv:1604.01148 [hep-ph]; A. Ahriche, K. L. McDonald and S. Nasri, arXiv:1604.05569 [hep-ph]; A. Ahriche, A. Manning, K. L. McDonald and S. Nasri, arXiv:1604.05995 [hep-ph]; E. Ma, N. Pollard, O. Popov and M. Zakeri, arXiv:1605.00991 [hep-ph]; T. Nomura, H. Okada and Y. Orikasa, arXiv:1605.02601

[hep-ph]; C. Hagedorn, T. Ohlsson, S. Riad and M. A. Schmidt, arXiv:1605.03986 [hep-ph]; O. Antipin, P. Culjak, K. Kumericki and I. Picek, arXiv:1606.05163 [hep-ph]; T. Nomura and H. Okada, Phys. Lett. B **761**, 190 (2016) [arXiv:1606.09055 [hep-ph]]; P. H. Gu, E. Ma and U. Sarkar, arXiv:1608.02118 [hep-ph]; S. Y. Guo, Z. L. Han and Y. Liao, arXiv:1609.01018 [hep-ph]; A. E. Carcamo Hernandez, arXiv:1512.09092 [hep-ph]; L. Megrelidze and Z. Tavartkiladze, arXiv:1609.07344 [hep-ph]; K. Cheung, T. Nomura and H. Okada, arXiv:1610.02322 [hep-ph];

[3] O. Seto and T. Shimomura, arXiv:1610.08112 [hep-ph].

[4] A. Zee, Nucl. Phys. B **264**, 99 (1986); K. S. Babu, Phys. Lett. B **203**, 132 (1988); K. S. Babu and C. Macesanu, Phys. Rev. D **67**, 073010 (2003) [hep-ph/0212058]; D. Aristizabal Sierra and M. Hirsch, JHEP **0612**, 052 (2006) [hep-ph/0609307]; M. Nebot, J. F. Oliver, D. Palao and A. Santamaria, Phys. Rev. D **77**, 093013 (2008) [arXiv:0711.0483 [hep-ph]]; D. Schmidt, T. Schwetz and H. Zhang, Nucl. Phys. B **885**, 524 (2014) [arXiv:1402.2251 [hep-ph]]; J. Herrero-Garcia, M. Nebot, N. Rius and A. Santamaria, Nucl. Phys. B **885**, 542 (2014) [arXiv:1402.4491 [hep-ph]]; H. N. Long and V. V. Vien, Int. J. Mod. Phys. A **29**, no. 13, 1450072 (2014) [arXiv:1405.1622 [hep-ph]]; V. Van Vien, H. N. Long and P. N. Thu, arXiv:1407.8286 [hep-ph]; M. Aoki, S. Kanemura, T. Shindou and K. Yagyu, JHEP **1007**, 084 (2010) [Erratum-ibid. **1011**, 049 (2010)] [arXiv:1005.5159 [hep-ph]]; M. Lindner, D. Schmidt and T. Schwetz, Phys. Lett. B **705**, 324 (2011) [arXiv:1105.4626 [hep-ph]]; S. Baek, P. Ko, H. Okada and E. Senaha, JHEP **1409**, 153 (2014) [arXiv:1209.1685 [hep-ph]]; M. Aoki, J. Kubo and H. Takano, Phys. Rev. D **87**, no. 11, 116001 (2013) [arXiv:1302.3936 [hep-ph]]; Y. Kajiyama, H. Okada and K. Yagyu, Nucl. Phys. B **874**, 198 (2013) [arXiv:1303.3463 [hep-ph]]; Y. Kajiyama, H. Okada and T. Toma, Phys. Rev. D **88**, 015029 (2013) [arXiv:1303.7356]; S. Baek, H. Okada and T. Toma, JCAP **1406**, 027 (2014) [arXiv:1312.3761 [hep-ph]]; H. Okada, arXiv:1404.0280 [hep-ph]; H. Okada, T. Toma and K. Yagyu, Phys. Rev. D **90**, no. 9, 095005 (2014) [arXiv:1408.0961 [hep-ph]]; H. Okada, arXiv:1503.04557 [hep-ph]; C. Q. Geng and L. H. Tsai, arXiv:1503.06987 [hep-ph]; S. Kashiwase, H. Okada, Y. Oriksa and T. Toma, arXiv:1505.04665 [hep-ph]; M. Aoki and T. Toma, JCAP **1409**, 016 (2014) [arXiv:1405.5870 [hep-ph]]; S. Baek, H. Okada and T. Toma, Phys. Lett. B **732**, 85 (2014) [arXiv:1401.6921 [hep-ph]]; H. Okada and Y. Oriksa, arXiv:1509.04068 [hep-ph]; D. Aristizabal Sierra, A. Degee, L. Dorame and M. Hirsch, JHEP **1503**, 040 (2015) [arXiv:1411.7038 [hep-ph]]; T. Nomura and

H. Okada, Phys. Lett. B **756**, 295 (2016) [arXiv:1601.07339 [hep-ph]]; T. Nomura, H. Okada and Y. Oriksa, arXiv:1602.08302 [hep-ph]; C. Bonilla, E. Ma, E. Peinado and J. W. F. Valle, arXiv:1607.03931 [hep-ph]; M. Kohda, H. Sugiyama and K. Tsumura, Phys. Lett. B **718**, 1436 (2013) [arXiv:1210.5622 [hep-ph]]; B. Dasgupta, E. Ma and K. Tsumura, Phys. Rev. D **89**, 041702 (2014) [arXiv:1308.4138 [hep-ph]]; T. Nomura and H. Okada, arXiv:1607.04952 [hep-ph]; T. Nomura and H. Okada, arXiv:1609.01504 [hep-ph].

- [5] L. M. Krauss, S. Nasri and M. Trodden, Phys. Rev. D **67**, 085002 (2003) [arXiv:hep-ph/0210389]; M. Aoki, S. Kanemura and O. Seto, Phys. Rev. Lett. **102**, 051805 (2009) [arXiv:0807.0361]; M. Gustafsson, J. M. No and M. A. Rivera, Phys. Rev. Lett. **110**, 211802 (2013) arXiv:1212.4806 [hep-ph]; A. Ahriche, S. Nasri and R. Soualah, Phys. Rev. D **89**, 095010 (2014) [arXiv:1403.5694 [hep-ph]]; A. Ahriche, C. S. Chen, K. L. McDonald and S. Nasri, Phys. Rev. D **90**, no. 1, 015024 (2014) [arXiv:1404.2696 [hep-ph]]; A. Ahriche, K. L. McDonald and S. Nasri, JHEP **1410**, 167 (2014) [arXiv:1404.5917 [hep-ph]]; H. Okada and Y. Oriksa, Phys. Rev. D **90**, no. 7, 075023 (2014) [arXiv:1407.2543 [hep-ph]]; H. Hatanaka, K. Nishiwaki, H. Okada and Y. Oriksa, Nucl. Phys. B **894**, 268 (2015) [arXiv:1412.8664 [hep-ph]]; L. G. Jin, R. Tang and F. Zhang, Phys. Lett. B **741**, 163 (2015) [arXiv:1501.02020 [hep-ph]]; P. Culjak, K. Kumericki and I. Picek, Phys. Lett. B **744**, 237 (2015) [arXiv:1502.07887 [hep-ph]]; H. Okada, N. Okada and Y. Oriksa, Phys. Rev. D **93**, no. 7, 073006 (2016) [arXiv:1504.01204 [hep-ph]]; C. Q. Geng, D. Huang and L. H. Tsai, Phys. Lett. B **745**, 56 (2015) [arXiv:1504.05468 [hep-ph]]; A. Ahriche, K. L. McDonald, S. Nasri and T. Toma, Phys. Lett. B **746**, 430 (2015) [arXiv:1504.05755 [hep-ph]]; K. Nishiwaki, H. Okada and Y. Oriksa, arXiv:1507.02412 [hep-ph]; H. Okada and K. Yagyu, arXiv:1508.01046 [hep-ph]; A. Ahriche, K. L. McDonald and S. Nasri, arXiv:1508.02607 [hep-ph]; Y. Kajiyama, H. Okada and K. Yagyu, JHEP **10**, 196 (2013) arXiv:1307.0480 [hep-ph]; S. F. King, A. Merle and L. Panizzi, arXiv:1406.4137 [hep-ph]; S. Kanemura, K. Nishiwaki, H. Okada, Y. Oriksa, S. C. Park and R. Watanabe, arXiv:1512.09048 [hep-ph]; H. Okada and K. Yagyu, Phys. Lett. B **756**, 337 (2016) [arXiv:1601.05038 [hep-ph]]; P. Ko, T. Nomura, H. Okada and Y. Oriksa, arXiv:1602.07214 [hep-ph]; T. Nomura, H. Okada and Y. Oriksa, arXiv:1603.04631 [hep-ph]; T. T. Thuc, L. T. Hue, H. N. Long and T. P. Nguyen, arXiv:1604.03285 [hep-ph]; D. Cherigui, C. Guella, A. Ahriche and S. Nasri, arXiv:1605.03640 [hep-ph]; T. Nomura, H. Okada and N. Okada, arXiv:1608.02694 [hep-ph]; K. Cheung, H. Ishida and H. Okada, arXiv:1609.06231

[hep-ph].

- [6] T. Nomura and H. Okada, Phys. Lett. B **755**, 306 (2016) [arXiv:1601.00386 [hep-ph]]; T. Nomura and H. Okada, arXiv:1601.04516 [hep-ph].
- [7] T. Nomura and H. Okada, Phys. Lett. B **761**, 190 (2016) [arXiv:1606.09055 [hep-ph]].
- [8] D. V. Forero, M. Tortola and J. W. F. Valle, Phys. Rev. D **90**, no. 9, 093006 (2014) [arXiv:1405.7540 [hep-ph]].
- [9] J. Herrero-Garcia, M. Nebot, N. Rius and A. Santamaria, Nucl. Phys. B **885**, 542 (2014) [arXiv:1402.4491 [hep-ph]].
- [10] A. M. Baldini *et al.* [MEG Collaboration], arXiv:1605.05081 [hep-ex].
- [11] J. Adam *et al.* [MEG Collaboration], Phys. Rev. Lett. **110**, 201801 (2013) [arXiv:1303.0754 [hep-ex]].
- [12] D. S. Akerib *et al.*, arXiv:1608.07648 [astro-ph.CO].
- [13] A. Arhrib, Y. L. S. Tsai, Q. Yuan and T. C. Yuan, JCAP **1406**, 030 (2014) [arXiv:1310.0358 [hep-ph]].
- [14] K. Griest and D. Seckel, Phys. Rev. D **43**, 3191 (1991).
- [15] J. Edsjo and P. Gondolo, Phys. Rev. D **56**, 1879 (1997) [hep-ph/9704361].
- [16] P. A. R. Ade *et al.* [Planck Collaboration], Astron. Astrophys. **571**, A16 (2014) [arXiv:1303.5076 [astro-ph.CO]].
- [17] G. W. Bennett *et al.* [Muon g-2 Collaboration], Phys. Rev. D **73**, 072003 (2006) [hep-ex/0602035].